Article

Ni^{2+} and Cu^{2+} Biosorption by EPS-Producing *Serratia plymuthica* Strains and Potential Bio-Catalysis of the Organo–Metal Complexes

Rocco Zanetti [1], Sarah Zecchin [1], Milena Colombo [1], Gigliola Borgonovo [1], Stefania Mazzini [1], Leonardo Scaglioni [1], Giorgio Facchetti [2], Raffaella Gandolfi [2], Isabella Rimoldi [2] and Lucia Cavalca [1,*]

1 Dipartimento di Scienze per gli Alimenti, la Nutrizione e l'Ambiente (DeFENS), Università degli Studi di Milano, Via Celoria 2, 20133 Milan, Italy
2 Department of Pharmaceutical Science, University of Milan, Via Venezian 21, 20133 Milan, Italy
* Correspondence: lucia.cavalca@unimi.it

Abstract: In this study, a biosorption system for nickel (Ni^{2+}) and copper (Cu^{2+}) removal by selected exopolymeric substance-producing bacterial strains was evaluated from the perspective of water remediation. A preliminary screening in a biofilm-based filtration system allowed the selection of two best-performing *Serratia plymuthica* strains for specific Ni^{2+} and Cu^{2+} removal from synthetic solutions, as well as the definition of the optimal growth conditions. Further tests were conducted in a planktonic cell system in order to evaluate: (i) the effect of contact time, (ii) the effect of initial metal concentration, and (iii) the effect of biomass dose. *S. plymuthica* strain SC3I(2) was able to remove 89.4% of Ni^{2+} from a 50 mg L^{-1} solution, and showed maximum biosorption capacity of 33.5 mg g^{-1}, while *S. plymuthica* strain As3-5a(5) removed up to 91.5% of Cu^{2+} from a 200 mg L^{-1} solution, yielding maximum biosorption capacity of 80.5 mg g^{-1}. Adsorption equilibria of both metals were reached within 30 min, most of the process occurring in the first 2–4 min. Only Ni^{2+} biosorption data were adequately described by Langmuir and Freundlich isothermal models, as Cu^{2+} was in part subjected to complexation on the exopolymeric substances. The capability of the exopolymeric substances to stably coordinate a transition metal as Cu^{2+} offers the possibility of the eco-friendly re-use of these new hybrid systems as catalysts for application in addition reaction of B$_2$(pin)$_2$ on α,β-unsaturated chalcones with good results. The systems formed by biomass and Ni^{2+} were instead evaluated in transfer hydrogenation of imines. The biosorption performances of both strains indicate that they have the potential to be exploited in bioremediation technologies and the obtained organo–metal complexes might be valorized for biocatalytic purposes.

Keywords: heavy metal; water remediation; biosorption; nickel; copper; *Serratia plymuthica*; EPS; biocatalysis

1. Introduction

Heavy metals can severely affect ecosystems, whether they are released directly or mobilized from natural sources [1]. The reasons for ecosystem damage lie in the intrinsic toxicity of heavy metals, in their non-biodegradability, and in the phenomena of bioaccumulation to which many of them are subjected [2]. These factors also threaten human health, with sources of exposure being food, water, air, medicines, phytosanitary, fuels, metal-coated materials, and many others [3]. The natural occurrence of nickel (Ni) in sulfide and laterite-type ores is increasingly exploited by humans for extracting and purifying the metal, and the process has been demonstrated to have a significant environmental impact [4]. Copper (Cu) occurs naturally as native metal and in many minerals including Cu sulfides, Cu sulfosalts, Cu carbonates, and Cu(I) and Cu(II) oxides. As with many heavy metals, both Ni and Cu may be subjected to acid drainage when a natural source or mine slag is exposed to oxygen and water, leading to downstream contamination [5].

Water and soils are typical environmental matrices subjected to the effects of discharging industrial waste rich in heavy metals. Preventing this type of contamination relies on

treating waste materials before releasing them. In recent decades, consistent efforts have been made to treat metal-contaminated wastewater to reduce its metal content. This is mainly achieved through chemical-physical processes, which have the disadvantage of being highly expensive and in turn having a significant environmental impact [1]. Moreover, the high cost of these processes combines with frequent inefficiency when metals are present in low concentrations, in the range of 1–100 mg L^{-1} [6,7]. The application of biosorbents for heavy metal sequestration from soil and water is a cheaper and more sustainable approach that has been successfully demonstrated by various research groups [8,9]. Biosorption may be simply defined as the removal of substances from a solution by biological material [10]. Apart from the removal of pollutants for environmental protection, the topic of biosorption has deserved research interest for the subsequent recovery and re-use of precious metals (gold, copper, etc.). Indeed, heavy metal sources are not renewable, and the natural reserves are slowly being consumed [11]. Considering that a hybrid catalyst arises from the combination of a metal ion as a source of catalytic activity with a natural structure with the function of ligand to complete its coordination sphere like in metalloproteins and metalloenzymes [12,13], the possibility to re-use these biosorption systems has inspired many research groups [14–16].

The most studied biosorbents belong to fungi, algae, agricultural residues, archaea, and bacteria [1]. The mechanisms involved in biosorption processes are adsorption, i.e., the adhesion of a gaseous, liquid, or condensed solid substance to a surface (the adsorbent) [17], ion exchange, where an ion present at the interface of a solid adsorbent with the surrounding gaseous or liquid phase is exchanged with another ion of similar charge [18], complexation, namely the combination of single atom groups, ions or molecules into one larger ion or molecule [19], or diffusion and transport of substances across cell membrane towards the inside of the cell [20]. More than one of these mechanisms can coexist; however, the surface chemistry of the biosorbent plays a prevalent role and is therefore studied primarily to characterize a biosorbent [10]. The functional groups containing S, N, O, and P are directly engaged in the binding of metals [21]. Strains displaying high extracellular polymeric substances (EPS) productivity are generally recognized as potentially effective biosorbents. In fact, it has been stated that EPS secondary and tertiary structures are pH-determined [22] and influence ionic exchange dynamics, including heavy metal sorption [23]. Finally, metal characteristics (namely electronegativity and ionic radius) were demonstrated to influence the sorption process [23]. Among the aforementioned, no defined factor or a combination of them has been recognized as a determinant for the performance of the biosorption process, and laboratory screening remains the ultimate procedure of assessment. It can be generally said that the more the microorganism's structure is complex, the higher will be the possibility of the cell capturing the metal [24]. The surface chemistry of the biosorbent is evaluated by making use of techniques such as IR, NMR, Raman spectroscopy, and FTIR [21], possibly providing a mechanistic explanation of biosorption processes. A simplified yet commonly employed method aims to characterize biosorbent surface properties via mathematical fitting of experimental data (from biosorption experiments) to empirical modeling of sorbent-sorbate interaction [10]. In the present study, two EPS-producing bacterial strains of *Serratia plymuthica* were selected and evaluated for their potential to remove cationic nickel (Ni^{2+}) and copper (Cu^{2+}) from water in a bioremediation perspective by comparing two different biosorption systems and assessing the effect of the contact time, the initial metal concentration, and the biomass dose on the biosorption process. Equilibrium data of sorption were analyzed according to Freundlich and Langmuir isotherms and the characteristic parameters for each isotherm were determined. The interaction between the bacterial EPS and Ni^{2+}/Cu^{2+} was monitored by NMR titration experiments in which aliquots of the metals were added to the EPS solution. Finally, the possible exploitation of the so-obtained hybrid organo-metallic complexes was assessed by initial bio-catalytic screening in two different types of catalyzed reactions on the basis of the biosorbed metal ion.

2. Materials and Methods

2.1. Bacterial Culture

The bacterial strains used in the present study were previously isolated from arsenic- and petroleum hydrocarbon-contaminated soils. They belong to three *Serratia plymuthica* strains As3-5a(5), SC3I(2), SC5II, and one *Stenotrophomonas* sp. strain 13a, according to 16S rRNA nucleotide sequence analyses. Minimal inhibitory concentration (MIC) of Ni^{2+} and Cu^{2+} was assessed in glucose-added tris minimal medium [25] in the presence of increasing concentrations of metals. For the four strains, MIC of Ni^{2+} and Cu^{2+} was equal to 5 and 7.5 mmol L^{-1}, respectively, thus showing a medium resistance level. They were preserved as glycerol stocks in the collection of the Department of Food, Environmental and Nutritional Sciences at the University of Milan.

2.2. Biomass Production

The strains were cultivated on Millers' LB agar plates and three-day biomass was used to prepare the pre-inoculum (20 mL of Millers LB broth in 100 mL flasks). Cells in exponential growth phase were then inoculated (0.5%, *v/v*) into 1 L flasks containing Millers' LB broth and incubated at 30 °C, under shaking at 100 rpm. The cells were harvested at different time steps up to 72 h and washed with phosphate buffer (1 M PK buffer, pH 7.2), and resuspended in bi-distilled water to target the biomass concentration. Biomass was quantified by direct cell counts in the Thoma chamber as well as dried biomass.

2.3. EPS Extraction and Quantification

A heating extraction method described by Morgan et al. [26] was modified according to Xia et al. [27] in order to separate the loosely bound EPS (LB-EPS) from the tightly bound EPS (TB-EPS) fractions. For each fraction, the polysaccharide content was determined according to the anthrone color blue–green method with glucose standard described by Dreywood [28], while the protein yield was assessed by using the Bradford assay [29].

2.4. EPS Nuclear Magnetic Resonance and Fourier-Transform Infrared Spectroscopy

Nuclear magnetic resonance (NMR) spectra of the EPS solutions were recorded at 25 °C using a Bruker AV 600 spectrometer (Bruker, Bremen, Germany) equipped with a TXI z-gradient probe operating at a frequency of 600.10 MHz for ^1H nucleus. 6–7 mg of EPS were dissolved in 550 μL of 99.96% D_2O, the pH was adjusted at 5.1 by a diluted solution of DCl. The EPS samples were centrifuged for 2 min, and the supernatants were put in 5 mm NMR tubes. The ^1H NMR spectra were acquired with 256 NS, 16 K points in resolution and calibrated on the residual water signal set at 4.78 ppm. Stock solution (0.15 mmoli mL^{-1}) of Cu^{2+} and Ni^{2+} were prepared by dissolving $CuCl_2$ and $NiCl_2$ in D_2O, pH 5.0. NMR titrations were performed by adding increasing amounts of metal to the EPS samples from 0 to 2.4 mM.

The functional groups of EPS were determined by Fourier transform infrared spectroscopy (FTIR) spectra performed with a Perkin Elmer (Waltham, MA, USA) FTIR Spectrometer "Spectrum One" in a spectral region between 4000 and 650 cm^{-1}, and they were analyzed using the transmittance technique with 32 scans per ion and 4 cm^{-1} resolution.

2.5. Biosorption Experiments

In the biofilm-based system, 4 mL of bacterial suspensions, prepared in bi-distilled water at $OD_{600\ nm}$ = 2, were deposited onto a 0.2 μm cellulose acetate filter (Millipore, Burlington, MA, USA). Metal solutions of $NiCl_2$ (50 mg L^{-1} Ni^{2+}) or $CuCl_2$ (200 mg L^{-1} Cu^{2+}), prepared in MilliQ water at pH of 6.62 and 5.03, respectively, were vacuum-forced across the biomass-activated filter.

Metal content of the flow through was analyzed by inductively coupled plasma—mass spectrometry (ICP-MS), as described in the paragraph below.

In the planktonic cell system, the biomass was resuspended in 4 mL of $NiCl_2$ (50 mg L^{-1} Ni^{2+}) or $CuCl_2$ (200 mg L^{-1} Cu^{2+}), prepared in MilliQ water at pH of 6.62

and 5.03, respectively, and stirred in plastic tubes at 100 rpm at 23 °C. The effect of contact time on metal biosorption was studied using 50 mg L^{-1} Ni^{2+} and 200 mg L^{-1} Cu^{2+} solutions in MilliQ water; samples were collected after 4, 15, 33, 48, and 60 min from initial contact. The effect of biomass dose was assessed by employing 1.20×10^9 to 2.73×10^{10} cells mL^{-1} of *Serratia plymuthica* strain SC3I(2) for Ni^{2+} biosorption and 7.75×10^8 to 7.43×10^{10} cells mL^{-1} of *Serratia plymuthica* strain As3-5a(5) for Cu^{2+} biosorption. The effect of the initial metal concentration and isothermal equilibrium parameters were assessed by testing 10, 20, 30, 40, and 50 mg L^{-1} Ni^{2+} and 40, 80, 120, 160, and 200 mg L^{-1} Cu^{2+} with constant biomass dose. Aliquots of the suspension were centrifuged for 3 min at 13300 rpm thus separating the adsorbent biomass from the supernatant, which was analyzed by ICP-MS.

Each experiment was conducted in triplicate and the abiotic controls were always analyzed.

2.6. Analytical Methods

The samples for Ni^{2+} and Cu^{2+} analysis were diluted and acidified with HNO$_3$ (final concentration of 2% (*v/v*)). The elements were measured by inductively coupled plasma mass spectrometry (ICP-MS, Agilent Technologies, Santa Clara, CA, USA), using a multi-standard solution (Agilent Technologies, Santa Clara, CA, USA).

The quantification of metal adsorbed by the biomass was obtained by the difference of metal flowed through the filter or the supernatant with respect to the metal initially supplied. The metal uptake by the biomass and equilibrium adsorption amount were expressed as

$$\%Removal = \frac{100(C_i - C_e)}{C_i} \tag{1}$$

and

$$q_e = \frac{V(C_i - C_e)}{W} \tag{2}$$

respectively, where C_i is the initial metal ion concentration (mg L^{-1}), C_e is the equilibrium concentration (mg L^{-1}), q_e (mg g^{-1}) is equilibrium adsorption amount (or biosorption capacity), V is the volume of the solution (L) and W is the amount of biomass (g).

On a sample basis, the metal content absorbed onto the biomass was directly measured, to ensure effectiveness of the determination by difference from flow-through and supernatant. For this purpose, the biomass was mineralized by microwave treatment (CEM, MARS5) in the presence of HNO$_3$.

2.7. Statistical Analysis

All experiments were conducted in triplicate and the results were expressed as means ± standard deviations. Statistical analyses were performed with Real Statistic Resource Pack release 8.2 (license Charles Zaiontz). One-way analysis of variance (ANOVA) was used to test for the significance between means ($p < 0.05$) followed by Tukey's test. Multiple comparisons of means-to-controls were performed according to Dunnett's test.

2.8. Adsorption Isotherms

Experimental data were described according to the Freundlich adsorption model, which defines adsorption to heterogeneous surfaces [10], i.e., surfaces possessing adsorption sites of varying affinities. The Freundlich isotherm equation is

$$q_e = K_f C_e{}^{\beta} \tag{3}$$

where K_f is the Freundlich constant (L g^{-1}), an affinity parameter estimating the bonding energy, and β is a heterogeneity parameter (the smaller the value of β, the greater the heterogeneity). Heterogeneity was also expressed with the parameter $n_F = 1/\beta$, whose value indicates the degree of non-linearity between solution concentration and adsorption as follows: if the value of n_F is equal to unity, the adsorption is linear; if the value is

below unity, the adsorption process is chemical; if the value is above unity, adsorption is a favorable physical process [30]. The linearized form of the Freundlich equation is

$$\log q_e = \log K_f + \beta \log C_e \tag{4}$$

Plotting $\log q_e$ versus $\log C_e$ allowed generating the intercept value of K_f and the slope β [30,31]. In addition to Freundlich isotherm, the Langmuir equation allowed for a simplified estimation of the maximum theoretical monolayer adsorption capacity by the biomass, defined according to the equation

$$q_e = Q_m K_l C_e / (1 + K_l C_e) \tag{5}$$

where Q_m is the maximum adsorption of sorbate (metal ions) per biomass unit (mg g^{-1}) and K_l (Langmuir constant, L g^{-1}) is an affinity parameter related to the bonding energy of the sorbate to the surface [32]. The Langmuir isotherm assumes that a finite number of uniform adsorption sites is present on the sorbent and that there is no lateral interaction between the adsorbed species [10]. The linearized form of the Langmuir isotherm is

$$\frac{C_e}{q_e} = \frac{1}{Q_m K_l} + \frac{C_e}{Q_m} \tag{6}$$

The plot of C_e/q_e versus C_e was used to obtain the value of Q_m from the slope $1/Q_m$ and the value of K_l from the intercept $1/Q_m K_l$. Comparing fitting goodness of experimental data with the two models provided basic information on metal-biosorbent affinity and sorbent surface properties. The essential feature of the Langmuir isotherm was expressed with the dimensionless constant R_L (separation factor, also called equilibrium parameter) which is defined by the equation

$$R_L = 1/(1 + a_L \, C_i) \tag{7}$$

where a_L (L mg^{-1}) is an expression of the value of the Langmuir constant with respect to the initial metal concentration; it is calculated as

$$a_L = K_l / Q_m \tag{8}$$

The value of R_L indicates the shape of the isotherms to be either unfavorable ($R_L > 1$), linear ($R_L = 1$), favorable ($0 < R_L < 1$) or irreversible ($R_L = 0$) [30].

2.9. General Procedure for Catalyzed Addition of Bis(Pinacolate)Diboron on (E)-3-(4-Chlorophenyl)-1-phenylprop-2-en-1-one

An amount of 1 eq. of substrate, 1.2 eq. of Bis(pinacolate)diboron (B$_2$(pin)$_2$) was placed in a round bottom flask and the Cu^{2+} catalyst (ratio 20:1=substrate:catalyst) was transferred into the flask with 5 mL of Et$_2$O. The reaction mixture was magnetically stirred at room temperature and after 15 h the suspension was centrifuged (6000 rpm, 10 min). The organic phase was concentrated under vacuum and the residue was dissolved with 4 mL of a THF/H$_2$O mixture (1.5:1), an excess of NaBO$_3$·H$_2$O was added, and the resulting mixture was stirred for 2 h at room temperature. The mixture was then extracted with EtOAc (5 mL × 3 times), the collected organic phases were dried over anhydrous Na$_2$SO$_4$ and the solvent was evaporated. The sample was analyzed by ^{1}H-NMR and HPLC analyses. HPLC conditions for 3-(4-chlorophenyl)-3-hydroxy-1-phenylpropan-1-one: Chiralcel AD; eluent hexane/iso-propanol = 90/10; λ = 240 nm; flow = 1.0 mL/min. Retention time for: S-isomer: 5.7 min, R-isomer: 8.5 min [33].

*2.10. General Procedure for Transfer Hydrogenation on 3-Methylbenzo[d]isothiazole 1,1-dioxide*

The substrate was dissolved in a 100 μL of buffer (MOPS 1.2 M, final pH = 7.8) and catalyst (2% mol) previously dissolved in DMF was added. Then, 15 eq. of HCOONa 3 M

was added as hydrogen source. The reaction was stirred for 18 h at 30 °C. At the end of the reaction, 10 µL of NaOH 10 N was added and the aqueous media was extracted with CH_2Cl_2. The organic layers were dried with Na_2SO_4, filtered and the solvent was evaporated. The conversion of 6,7-dimethoxy-1-methyl-1,2,3,4-tetrahydroisoquinoline was determined by HPLC equipped with Chiralcel OD-H column: eluent hexane/iso-propanol = 80/20; λ = 220 nm; flow = 0.7 mL/min; retention time for: t(1°ent) = 19.5 min; t(2°ent) = 24.6 min [34].

3. Results and Discussion

3.1. Metal Adsorption in the Biofilm-Based System

In the biofilm-based system, three *Serratia plymuthica* strains As3-5a(5), SC3I(2), SC5(II), and one *Stenotrophomonas* sp. strain 13a were tested for their capability of removing Ni^{2+} and Cu^{2+} from water solutions, as a function of cell growth phase according to different incubation times (Figure 1).
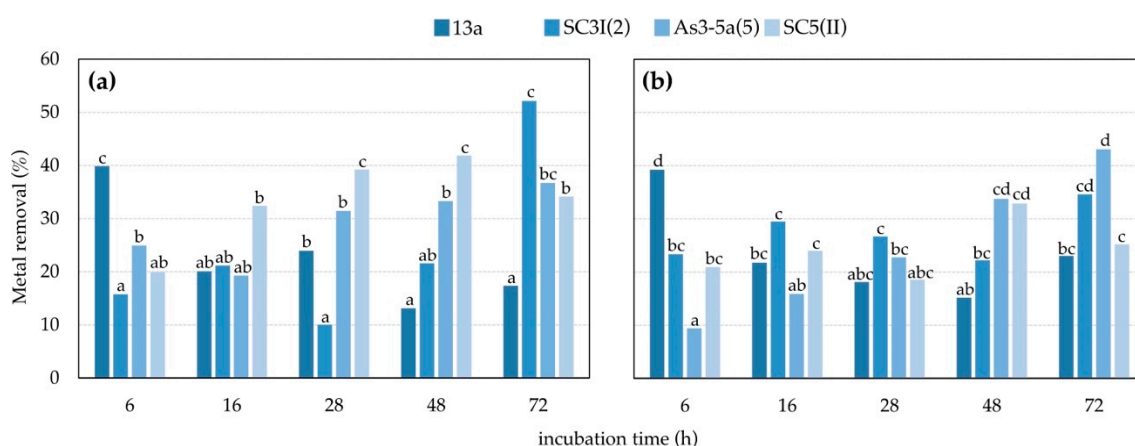

Figure 1. Effect of incubation time on biosorption of Ni^{2+} (**a**) and Cu^{2+} (**b**) by different strains in the biofilm-based system. Letters indicate whether the values differ significantly according to Tukey's test ($p < 0.05$).

The strains were selected for further study, according to adsorption data obtained from a larger preliminary screening [34]. Ni^{2+} removal increased as a function of the growth phase of *S. plymuthica* strains SC3I(2) and As3-5a(5), whereas it was the opposite for *Stenotrophomonas* sp. strain 13a which displayed higher removal with six-hour-grown cells.

Additionally, Cu^{2+} removal by the mentioned strains followed a similar pattern to that of Ni^{2+}, according to the cell growth phase, while *S. plymuthica* strain SC5(II) was the only one displaying higher Ni^{2+} and Cu^{2+} removal when cells were grown for 48 h. The highest removal of Ni^{2+} from 50 mg L^{-1} solution was 52.2% and it was obtained by *S. plymuthica* strain SC3I(2) after 72 h incubation, while the highest removal of Cu^{2+} from 200 mg L^{-1} solution was 43.1% and it was achieved by *S. plymuthica* strain As3-5a(5), when cells were grown for 72 h. The biosorption capacity of Ni^{2+} and Cu^{2+} by strains SC3I(2) and As3-5a(5) was 5.2 mg g^{-1} and 18.3 mg g^{-1}, respectively. Due to these characteristics, the two strains were further characterized.

3.2. EPS Production

The amount of EPS produced by the two *S. plymuthica* strains was measured at 48 h and 72 h (Figure 2). Strain As3-5a(5) produced more EPS than strain SC3I(2), and the EPS amount was higher after 48 h growth than 72 h. On the contrary, EPS production by strain SC3I(2) was slightly higher after 72 h growth.
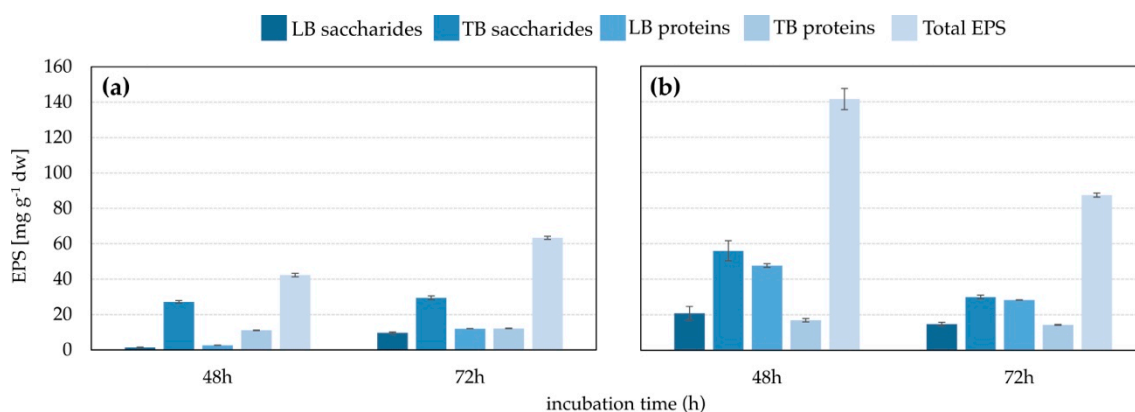
Figure 2. EPS production as a function of incubation time by *S. plymuthica* strain SC3I(2) (**a**) and *S. plymuthica* strain As3-5a(5) (**b**).

3.3. Analysis of the Interaction of EPS with Metals by NMR

The ^{1}H NMR spectrum of EPS provides information about α and β anomeric protons region (5.8–4.2 ppm) as well as C2 and C6 ring proton region (3.1–4.5 ppm). In the spectrum of EPS of strain As3-5a(5), six intense signals in the anomeric region at 5.39, 5.24, 5.02, 4.49, 4.44, and 4.27 ppm were observed (Figure 3). The spectrum of EPS of the SC3I(2) strain showed a similar NMR profile. Signals between 2.3 and 1.2 ppm were attributed to methylated groups of 6-deoxy and acetyl sugars.
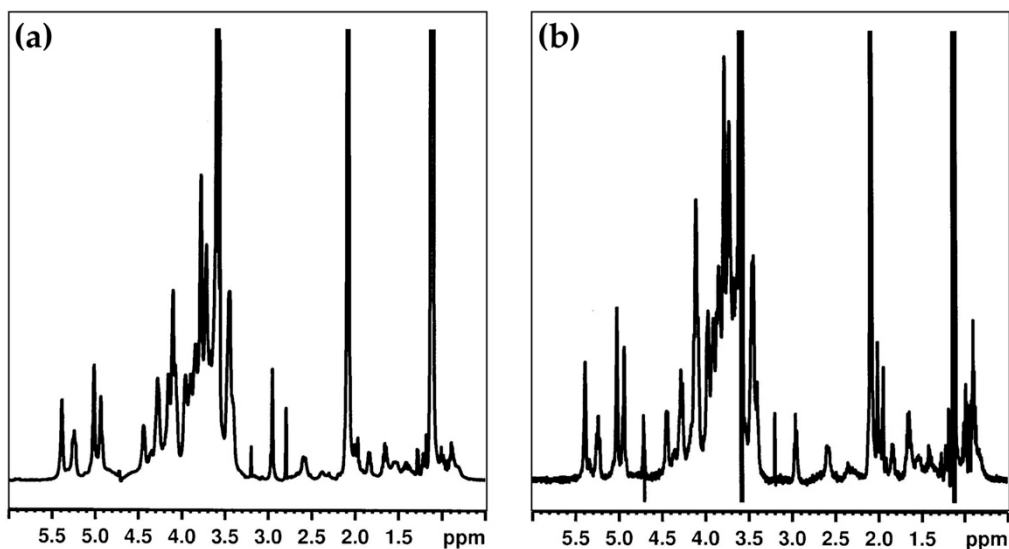

Figure 3. ^{1}H NMR spectra of EPS extracted from *S. plymuthica* strain SC3I(2) (**a**) and *S. plymuthica* strain As3-5a(5) (**b**) in D$_2$O, pH 5.1, T = 25 °C.

The functional groups of EPS extracted from *S. plymuthica* strains As3-5a(5) and SC3I(2) were determined by FTIR (Supplementary Figures S1 and S2). The spectra of the two strains showed a similar profile. Particularly, FTIR analysis displayed a broad and strong band at 3278 cm^{-1} due to the stretching of O−H; the peak at 2925 cm^{-1} was attributable to C−H stretching. A peak at 1625 cm^{-1} was assigned to C=O and C=C stretching. The band at 1531 cm^{-1} was associated with the N−H bending in proteins, while the band at 1454 cm^{-1} was attributed to the stretching of C=O in COO^{-}. The peak at 1392 cm^{-1} could be attributed to S-O stretching, whereas the peak at 1239 cm^{-1} was indicative of stretching vibration of N-H and C-N bending. The band at 1062 cm^{-1} is attributed to asymmetric stretching of S=O and C-O C-H stretching of polysaccharides. The fingerprint region below 1000 cm^{-1}

suggested the existence of both α and β configuration at the anomeric carbon in accordance with FTIR spectra of previously reported bacterial EPS [22,35].

The interaction between the EPS of *S. plymuthica* strains SC3I(2) and As3-5a(5) with Ni^{2+} and Cu^{2+} was monitored by titration experiments in which aliquots of metal were directly added to the EPS solution inside the NMR tubes. No ^1H NMR spectral changes were detected by the addition of Ni^{2+} to EPS of strain SC3I(2); only irrelevant broadening could be observed at 2.4 mmol L^{-1} of metal addition (Figure 4).
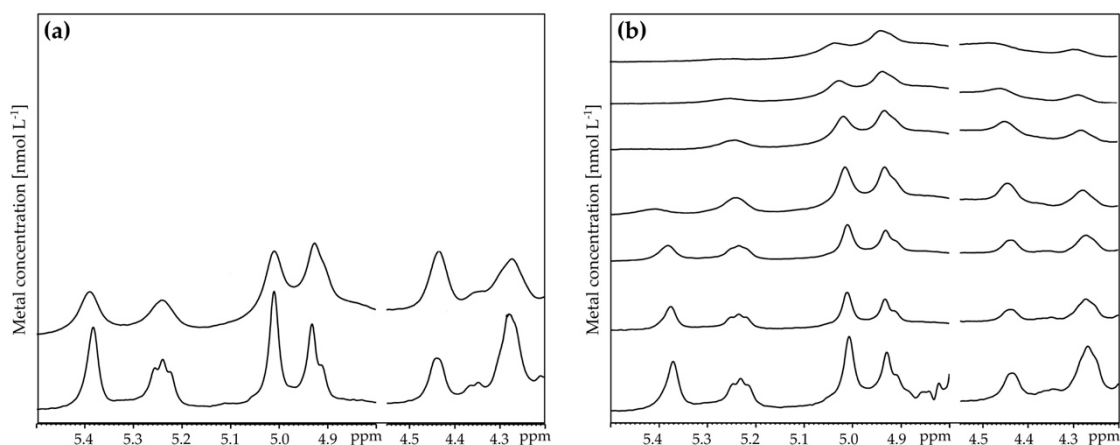
Figure 4. H NMR spectra of EPS-SC3I(2) in D_2O in presence of increased amounts of Ni^{2+} (**a**) and Cu^{2+} (**b**), pH 5.1, T = 25 °C.

After the addition of Cu^{2+} solution, small differences were detected in the NMR spectra of EPS of *S. plymuthica* strain SC3I(2) at 0.6 mmol L^{-1} Cu^{2+}. The broad anomeric protons at 5.41 and 5.24 ppm were still visible in the EPS of SC3I(2) strain at 0.9 mmol L^{-1}. Upon the addition of Ni^{2+} solution to EPS of strain As3-5a(5) a remarkable line broadening starting from 0.6 mmol L^{-1} of Ni^{2+} was observed (Figure 5).
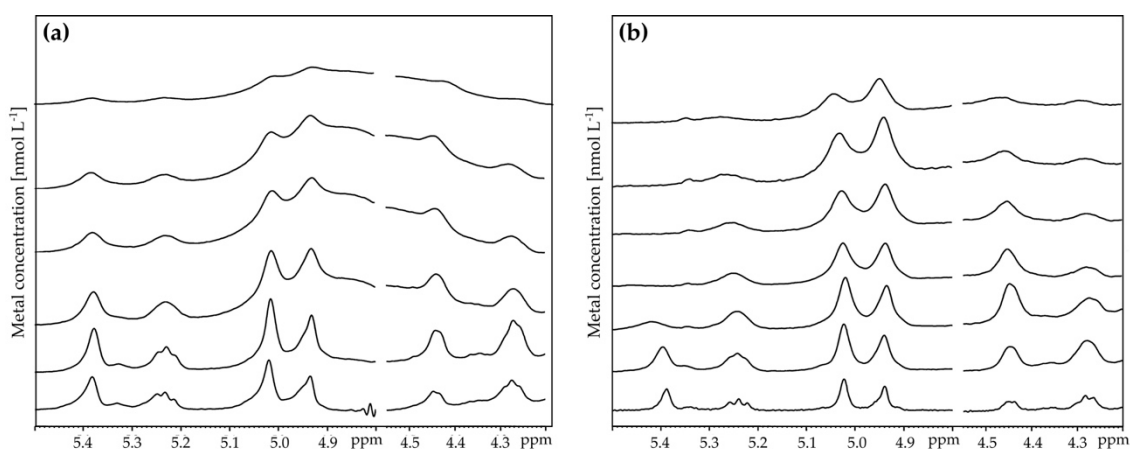
Figure 5. H NMR spectra of EPS-As3-5a(5) in D_2O in presence of increased amounts of Ni^{2+} (**a**) and Cu^{2+} (**b**), pH 5.1, T = 25 °C.

All the anomeric protons experienced a line broadening, and they were just barely visible at 2.4 mmol L^{-1} of Ni^{2+}. The water signal was very large due to the metal effect. Upon the addition of 0.3 mmol L^{-1} Cu^{2+} solution to the EPS of strain As3-5a(5), a generalized broadening and a moderate shift in the ^1H NMR anomeric signals were observed. The signal at 5.39 ppm moved downfield (Δδ = 0.07) and completely disappeared after the addition of 0.9 mmol L^{-1} Cu^{2+}. The same occurred for the signal at 5.24 ppm, which became very broad at 2.4 mmol L^{-1} Cu^{2+} (Δδ = 0.03). The signals at the up-field region

remained unaffected or exhibited insignificant variations for all the considered samples. It is possible to argue that complexation to EPS is the main mechanism responsible for Cu adsorption to EPS in strain As3-5a(5).

FTIR and NMR analysis underlined the heterogeneous characteristics of EPS, composed mostly of polysaccharides and proteins, in accordance with spectra obtained by previous studies [22]. The analyzed EPS contain various weak acid functions (carboxylic, phosphoryl, amide, amino, and hydroxyl groups) which ionize and that apparently participate in metal binding thanks to their negative charge and abundant availability. Particularly, at the acidic pH conditions of the present study, functional groups might be denser and more prone to adsorb heavy metals [22]. In addition to the metal–proton exchange, other mechanisms might be involved in the adsorption of metals by EPS, such as electrostatic interactions, cation exchange, and precipitation. Fang et al. [36] indicated the alcoholic, carboxylic, amino, and sulfate groups as responsible for the metal binding by EPS.

3.4. Cell Metal Adsorption: Effect of Contact Time

Ni^{2+} and Cu^{2+} adsorption to *S. plymuthica* strains SC3I(2) and As3-5a(5) as a function of contact time was evaluated in a planktonic system.

Rapid metal removal was measured 4 min after contact, followed by gradual uptake until an equilibrium was reached within 30 min, regardless of cell concentration (Figure 6).
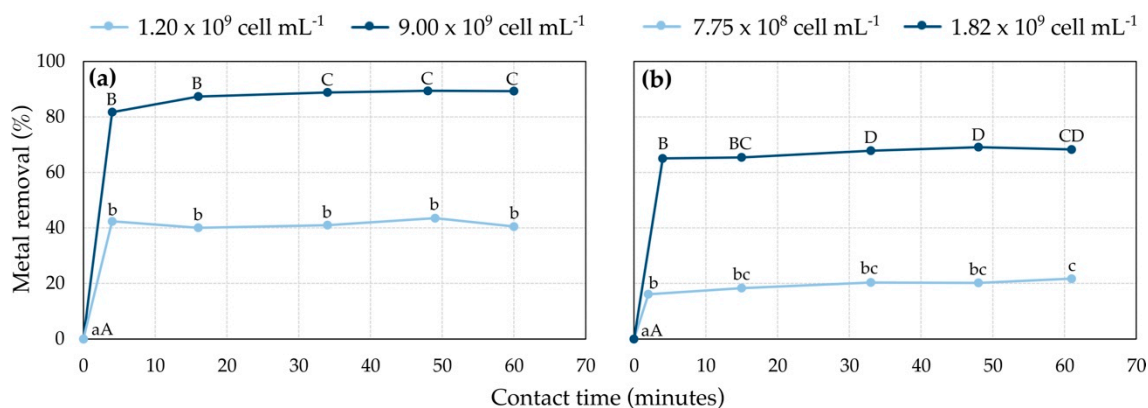

Figure 6. Effect of contact time on biosorption of Ni^{2+} (**a**) onto *S. plymuthica* strain SC3I(2) and Cu^{2+} (**b**) onto *S. plymuthica* strain As3-5a(5) biomass (initial Ni^{2+} concentration, 50 mg L^{-1}; initial Cu^{2+} concentration, 200 mg L^{-1}; temperature, 24 °C; agitation rate, 100 rpm). Letters indicate whether the values differ significantly according to Tukey's test ($p < 0.05$).

Cell number strongly influenced metal adsorption percentages, which were higher in the presence of higher cell numbers. The contact time of equilibrium is a crucial characteristic of biosorbents for both designing further adsorption experiments and because it strongly affects their potential transposition into effective full-scale bioremediation systems. The trend observed in the present study is similar to many others previously observed among biosorption systems of Ni^{2+} [37,38] and Cu^{2+} [31,39,40], although the equilibrium contact time found in previous studies was much longer, from a few hours to days [38,41,42]. Since short contact time is preferable, *S. plymuthica* strains SC3I(2) and As3-5a(5) deserve further study.

3.5. Cell Metal Adsorption: Effect of Initial Metal Concentration

The biosorption capacity of *S. plymuthica* strain SC3I(2) towards Ni^{2+} was evaluated by applying a constant biomass dose of 2.73×10^{10} cell mL^{-1}. Ni^{2+} biosorption capacity showed a linear increase with respect to the initial metal concentration: 0.67 mg g^{-1} cell d.w. and 2.95 mg g^{-1} cell d.w. were adsorbed being the initial Ni^{2+} concentration of 10 mg L^{-1} and 50 mg L^{-1}, respectively (Figure 7).
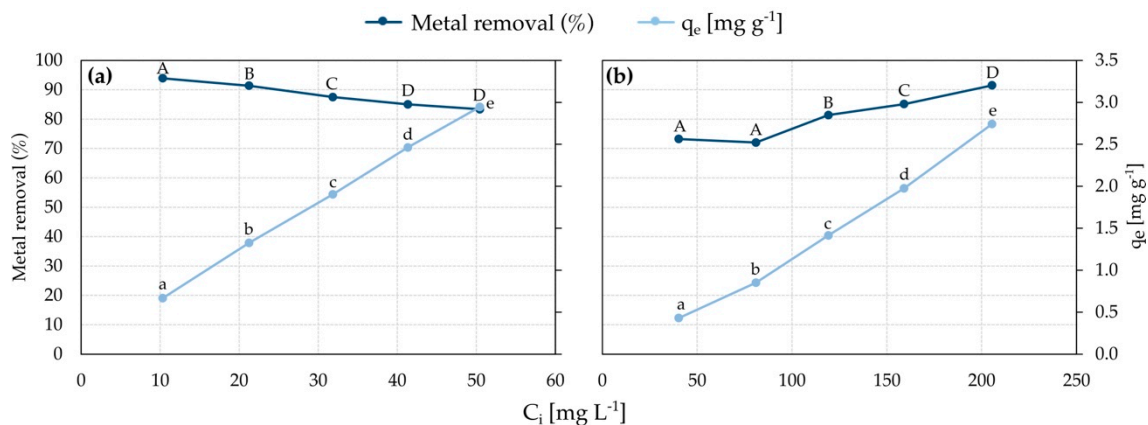
Figure 7. Effect of the initial metal concentration on biosorption capacity and removal of Ni^{2+} (**a**) by *S. plymuthica* strain SC3I(2) and Cu^{2+} (**b**) by *S. plymuthica* strain As3-5a(5) (SC3I(2) amount of biomass, 2.73×10^{10} cell mL^{-1}; As3-5a(5) amount of biomass 7.43×10^{10} cell mL^{-1}; temperature, 24 °C; agitation rate, 100 rpm; contact time, 30 min). Letters indicate whether the values differ significantly according to Tukey's test ($p < 0.05$).

This result can be explained by the presence of available and unoccupied binding sites when the metal is present at low concentrations; at higher metal concentrations, the sorbent–sorbate interaction is expected to increase, and resulted in higher biosorption capacity. Under the tested conditions, biosorption capacity is also expected to reach a plateau related to sorbent saturation. Contextually, the efficacy of the sorption process decreased, metal removal lowering from 93.9% to 83.4%. A probable explanation of this result is the increasing competition of metal ions for the available sites on biomass, as reported in other heavy metal biosorption studies [31,40,43]. Interestingly, Kashyap et al. [42] reported that Ni^{2+} biosorption on abundant bacterial biomass might result in a non-limiting amount of binding sites, showing higher removal when the initial metal concentration increases.

The biosorption capacity of *S. plymuthica* strain As3-5a(5) towards Cu^{2+} was evaluated by applying a constant biomass dose of 7.43×10^{10} cell mL^{-1}. Biosorption capacity showed a linear increase with respect to the initial metal concentration; 0.43 mg g^{-1} cell d.w. and 2.74 mg g^{-1} cell d.w. were adsorbed with an initial metal concentration of 40 mg L^{-1} and 205 mg L^{-1}, respectively. As for Ni^{2+} biosorption, such a result may be explained by the presence of unoccupied binding sites at low initial metal concentrations, meaning that the sorbent is unsaturated. In fact, the higher initial metal concentration was associated with higher biosorption capacity. As opposed to Ni^{2+} biosorption, Cu^{2+} removal percentage gradually increased from 73.2% to 91.5% with the initial metal concentration of 40 mg L^{-1} and 205 mg L^{-1}, respectively. A similar trend in both metal removal and biosorption capacity was observed in Cu^{2+} biosorption by *Micrococcus luteus* DE2008 [44]. As suggested by NMR, *S. plymuthica* strain As3-5a(5) EPS titration with Cu^{2+} evidenced an influence on several signals suggesting an efficient interaction with more binding sites. On the contrary, the EPS from *S. plymuthica* strain SC3I(2) did not show spectral changes as a consequence of the titration with Ni^{2+}, indicating a low binding affinity with this metal.

3.6. Cell Metal Adsorption: Effect of Biomass Dose

Assessing the effect of biomass dose on the biosorption process allows for identifying the conditions under which metal removal is maximized and for establishing the minimum quantity of biomass required to remove the metal from the solution at defined conditions [31,40].

Ni^{2+} removal by strain SC3I(2) increased when varying biomass dose from 7.10×10^{8} to 9.00×10^{9} cell mL^{-1}, resulting in 5.40% and 89.44%, respectively (Figure 8).
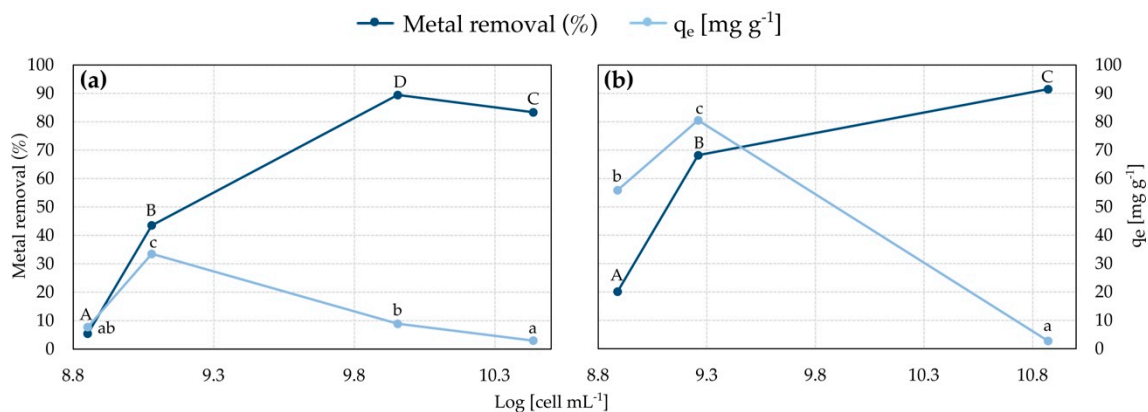
Figure 8. Effect of biomass dose on biosorption capacity and removal of Ni^{2+} (**a**) by *S. plymuthica* strain SC3I(2) and Cu^{2+} (**b**) by *S. plymuthica* strain As3-5a(5) (initial Ni^{2+} concentration, 50 mg L^{-1}; initial Cu^{2+} concentration, 200 mg L^{-1}; temperature, 24 °C; agitation rate, 100 rpm; contact time, 30 min). Letters indicate whether the values differ significantly according to Tukey's test ($p < 0.05$).

Further biomasses increase to 2.73×10^{10} produced a slightly lower metal removal (83.35%). The biosorption capacity had a peak of 33.50 mg g^{-1}dw, obtained when employing 1.2×10^9 cell mL^{-1}, while higher and lower biomass doses resulted in significantly lower ($p < 0.05$) biosorption capacity. Similarly, Cu^{2+} removal increased along with the increase in biomass dose; only 20.16% of metal was removed employing 7.75×10^8 cell mL^{-1}, and the removal increased to 91.5% with 7.43×10^{10} cell mL^{-1} of biomass dose. The highest biosorption capacity was 80.51 mg g^{-1}, obtained with 1.82×10^9 cell mL^{-1}; higher and lower biomass dose resulted in significantly lower ($p < 0.05$) biosorption capacity.

Over the years, several bacterial biosorbents have been evaluated for the removal of heavy metals, including Cu^{2+} and Ni^{2+} [1,21]. Although exhaustive comparison among biosorbents intrinsically lacks standardized experimental condition among biosorption systems [10], data on adsorption capacity and metal removal still provide a synthesis of biosorbent properties relevant to the remediation perspective. For example, strains of *Bacillus cereus* were demonstrated to adsorb up to 146.25 mg g^{-1} metal from a 250 mg L^{-1} Ni^{2+} solution, yielding 65% removal [45], or modified and immobilized *B. cereus* adsorbed 125 mg g^{-1} from 400 mg L^{-1} Ni^{2+} solution, yielding 82% removal [46]. Instead, *Sporosarcina pasteurii* strain 586S and *Bacillus megaterium* strain 1295S adsorbed 196.4 and 200.2 mg g^{-1} metal from 0.1–0.8 mg L^{-1} Ni^{2+} solutions, with maximum metal removals of 75.51% and 91.34%, respectively [47]. These results are referred to as the highest known Ni^{2+} bacterial biosorbents, as resumed by recent literature [1]. In the past, it was stated that the biosorption capacity for application to technology needs to be more than 150 mg g^{-1} [48], but biosorption is often positively evaluated for lower biosorption capacity (even <10 mg g^{-1}), especially when a good metal removal is met. Indeed, a relatively low adsorption capacity may be acceptable if a high biomass dose can overcome such limitation, providing good metal removal. As biomass production is a relevant cost in the bioremediation process [21], higher biosorption capacity would still be preferable, especially if the biosorbent requires specific culturing. Among the highest known Cu^{2+} bacterial biosorbents, *Micrococcus luteus* strain DE2008 showed removing 408 mg g^{-1} metal from 80.24 mg L^{-1} solution [44], i.e., a biosorption capacity five times higher than that of *S. plymuthica* strain As3-5a(5) tested in this study. However, as only 25% of metal was removed by *M. luteus* strain DE2008, *S. plymuthica* strain As3-5a(5) may result more suitable from a remediation perspective. Apart from the *M. luteus* strain DE2008, bacterial biosorbents generally showed less than 100 mg g^{-1} biosorption capacity for Cu^{2+} [1,21]; therefore, *S. plymuthica* strain As3-5a(5) must be considered a performing biosorbent worthy of further investigation. Interestingly, *Serratia marcescens* strain 16 was recently employed in a biosorption study, displaying biosorption capacity of 11.4 mg g^{-1} and 8.6 mg g^{-1} towards Ni^{2+} and Cu^{2+}, respectively [49], and *S. marcescens* was previously described as a possible bioaccumulator

and bioindicator for other heavy metals (Pb, Cd, and Cr) [50]. In the present study, the potential of the genus *Serratia* in the field of bioremediation is confirmed and supported by the strain-specific biosorption properties.

Strain SC3I(2) was also tested for Cu^{2+} removal, which was 87.1% Cu^{2+} with a biomass dose of 7.43×10^{10} cell mL^{-1}, slightly lower than removal by As3-5a(5) in the same conditions. Instead, strain As3-5a(5) was able to remove 70.9% Ni^{2+} with a biomass dose of 2.73×10^{10} cell mL^{-1}, lower than SC3I(2) in the same conditions. This result indicates that Cu^{2+} and Ni^{2+} removal are not restricted to only one of the selected *S. plymuthica* strains, but the specificity that was observed in the biofilm-based system was also confirmed in the planktonic cell system.
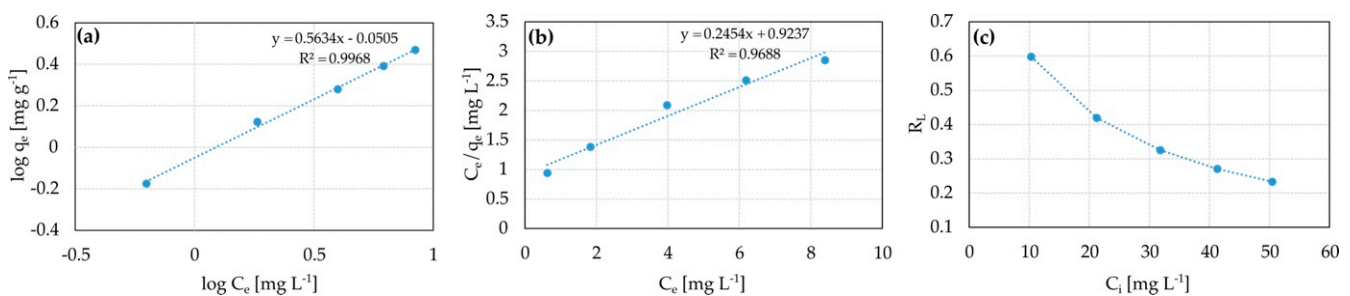
3.7. Adsorption Isotherms

Freundlich and Langmuir biosorption isotherms were used to determine sorbate-sorbent affinity and the most relevant surface properties of the sorbent. Ni^{2+} biosorption on *S. plymuthica* strain SC3I(2) was characterized by the values of the Freundlich constant K_f and the heterogeneity parameters β and n_F (Table 1).

Table 1. Summary of the Freundlich and Langmuir isotherm constants and comparison of linear regression coefficients of determination.

Sorption System.	Model Isotherm	Parameters	R^2
Ni^{2+}—*S. plymuthica* SC3I(2)	Freundlich	$K_f = 0.89$(L g^{-1}), ß = 0.50, $n_F = 1.98$	0.9968
	Langmuir	$Q_m = 4.1$ (mg g^{-1}), $K_l = 0.27$(L g^{-1}), $a_l = 0.07$(L mg^{-1}), $R_L = 0.23 - 0.60$	0.9688
Cu^{2+}—*S. plymuthica* As3-5a(5)	Freundlich	nd [1]	0.3789
	Langmuir	nd	0.0528

Note: [1] not determined.

The isotherm was found to be linear over the entire studied concentration range (10–50 mg L^{-1}) with a good correlation coefficient ($R^2 = 0.9968$) (Figure 9).

Figure 9. Adsorption isotherms for Ni^{2+} by *S. plymuthica* strain SC3I(2): Freundlich isotherm (**a**), Langmuir isotherm (**b**), and Langmuir separation factor (**c**) (amount of biomass, 2.73×10^{10} cell mL^{-1}; initial Ni^{2+} concentration, 50 mg L^{-1}; temperature, 24 °C; agitation rate, 100 rpm; contact time, 30 min).

Sorption data were also analyzed according to the linear form of the Langmuir isotherm, which yielded a linear correlation coefficient $R^2 = 0.9688$, slightly lower than that of the Freundlich model. The monolayer saturation capacity Q_m, Langmuir K_l, and a_l constants and the separation factor R_l obtained from the linear plot of C_e/q_e versus C_e are reported in Table 1. The higher R^2 resulting from the fit of experimental data to the Freundlich model suggests that the sorbent surface is mostly heterogeneous, having adsorption sites with different structures and binding energies. Additionally, the formation of a multilayer of sorbate particles is more probable than the formation of a monolayer, which is an assumption of the Langmuir isotherm. Heterogeneity is a coherent property of the bacterial surface and the EPS produced by *S. plymuthica* strain SC3I(2) are likely to give

a contribution. However, based on R^2 values, the linear form of both isotherms appears to produce a reasonable adsorption model. According to both models, Ni^{2+} adsorption on *S. plymuthica* strain SC3I(2) is a favorable process. In fact, the value of the Freundlich parameter above unity ($n_F = 1.98$) indicates that adsorption is a favorable physical process [30], and values of the Langmuir separation factor R_L (in the range 0–1) confirm the favorableness of adsorption, with higher R_L values at lower metal concentration indicating that adsorption is more favorable in such condition, in accordance with experimental metal removal percentages. At the tested conditions, the extrapolated monolayer saturation capacity Q_m accounts for 4.1 mg g^{-1}, which is far lower than the biosorption capacity that was determined experimentally (33.50 mg g^{-1}). Critical issues of considering Langmuir Q_m for estimating the maximum adsorption capacity concern reaching actual saturation of the sorbent in the experimental system [51]; low initial metal concentrations may lead to the elaboration of an incomplete and unsaturated isotherm, therefore underestimating maximum adsorption capacity. In addition, Q_m is referred to as a monolayer adsorption system and does not take into account the effect of adsorbed ions on a multilayer system.

Experimental data of Cu^{2+} biosorption by *S. plymuthica* strain As3-5a(5) yielded very low fit to both Langmuir and Freundlich isotherms, R^2 being 0.0528 and 0.3789, respectively. Some Langmuir isotherm assumptions are likely disregarded, namely surface homogeneity and monolayer structure of adsorbed ions; it was reported that the Langmuir model is used extensively providing successful representation of experimental data when these assumptions are met [52], hence, Cu^{2+} biosorption on *S. plymuthica* strain As3-5a(5) does not meet at least one of the mentioned conditions. The R^2 resulting from the fit of the experimental data to the Freundlich model indicates a slightly better correspondence than that of Langmuir. However, one or more assumptions of the Freundlich isotherm may have not occurred [53]. The important role of EPS for heavy metals removal had already been recognized; for example, the EPS produced by a *Pseudomonas putida* X4 adsorbed up to 169.24 mg g^{-1} Cu, which was higher than the cells [54], and it was observed that glycoconjugates of EPS can provide most of the sorption sites for heavy metals, including Cu [55]. Based on data obtained in the present study, the removal of Cu^{2+} obtained by strain As3-5a(5) could be exploited for a substantial improvement of the metal removal process.

3.8. Catalytic Experiments

The catalytic screening for both the strains with a metal ion (Cu^{2+} and Ni^{2+}) was evaluated in two different well-known catalyzed reactions in which the metal complexes generally work well as catalysts (Figure 10).
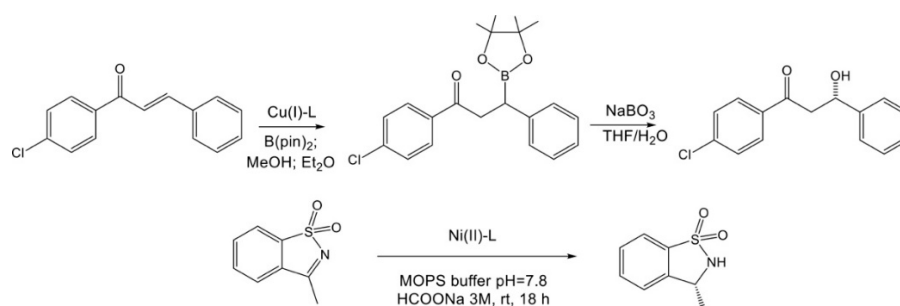
Figure 10. Catalytic reactions for Cu^{2+}— and Ni^{2+} —biomass hybrid catalysts.

For the hybrid systems obtained with biosorbed Cu^{2+} ion, the results of the 1,4-conjugate addition to the carbon–carbon double bond were in accordance with previously obtained using as ligand two different *Serratia* [33]. The new C–B bond using bis(pinacolato)diboron (B$_2$(pin)$_2$), which is one of the most practical tools for this reaction, was obtained via transition metal catalysis. When the hybrid system was formed by the coordination of Cu^{2+} with As3-5a(5), a 58 % conversion was obtained with promising enantiomeric excess of 18 %, as in our previous work with other different two strains as ligands. The fact that

an enantiomeric excess was achieved underlines the asymmetric nature of the interaction between the substrate and the catalyst arising from the chiral coordination sphere by EPSs. Additionally, in the case of SC3I(2), a 53 % conversion and 11 % e.e. were observed, confirming the nature of the coordination between *Serratia* strains with Cu^{2+}. On the contrary, the transfer hydrogenation with the corresponding Ni^{2+}-complexes did not afford the product if not in traces (less than 8 %) for both the strains employed as ligands.

4. Conclusions

In the present study, two EPS-producing *Serratia plymuthica* strains were identified and tested for Ni^{2+} and Cu^{2+} removal from water solutions in a planktonic-cell biosorption system. The process resulted dependent on bacteria growth conditions, cell metal contact time, initial metal concentration, and biomass dose. For both metals, sorption equilibrium was reached within 2–4 min. In a 50 mg L^{-1} Ni^{2+} solution the highest metal removal and biosorption capacity were 89.4% and 33.5 mg g^{-1}, achieved by the *S. plymuthica* strain SC3I(2), while 91.5% metal removal and 80.5 mg g^{-1} biosorption capacity were achieved by the *S. plymuthica* strain As3-5a(5) in a 200 mg L^{-1} Cu^{2+} solution. Ni^{2+} biosorption data were adequately described by both Freundlich ($R^2 = 0.9968$) and Langmuir ($R^2 = 0.9688$) isothermal models, which confirmed the spontaneity and favorableness of the process, while Cu^{2+} biosorption data yielded very low fit to these models. The EPS produced by bacterial strains were quantified and analyzed by NMR in response to metal titration and functional groups identified by FTIR; a very small interaction was detected between Ni^{2+} and the SC3I(2) EPS, while in the As3-5a(5) EPS titrated with Cu^{2+} a generalized broadening and moderate shifts in the anomeric signals were observed. These data indicate that complexation is conceivable for Cu^{2+} biosorption by strain As3-5a(5) and excludible for Ni^{2+} biosorption by strain SC3I(2). FTIR and NMR analyses underlined the heterogeneous characteristics of EPS, composed mostly of polysaccharides and proteins, that would participate in metal-binding thanks to their negative charge. A metal–proton exchange mechanism might occur, although other mechanisms, such as electrostatic interactions and precipitation, cannot be excluded. Both strains also displayed promising bio-catalytic properties as organo–metal complexes when the biomass was subjected to Cu^{2+} biosorption, suggesting the possibility of re-using the bacterial sorbent as a precious material. On the other hand, the organo–Ni^{2+} complexes were not shown to have satisfactory catalytic properties. Results of the present study indicate that the *S. plymuthica* strains SC3I(2) and As3-5a(5) have good potential for being exploited as biosorbents in a water remediation perspective, with the advantage of possibly obtaining a useful product rather than a waste product, in the case of Cu^{2+} biosorption. If the organo–Ni^{2+} complexes will not demonstrate catalytic properties, the "bio-recovery" of metal (i.e., desorbing it from biomass) might be a sustainable way to recover this non-renewable material.

Author Contributions: Conceptualization, L.C. and R.Z.; funding acquisition, L.C.; reading and approval of the published version of the manuscript, R.Z., S.Z., M.C., G.B., S.M., L.S., G.F., R.G., I.R. and L.C. All authors have read and agreed to the published version of the manuscript.

Data Availability Statement: Not applicable.

Conflicts of Interest: The authors declare no conflict of interest.

References

1. Rana, A.; Sindhu, M.; Kumar, A.; Dhaka, R.K.; Chahar, M.; Singh, S.; Nain, L. Restoration of heavy metal-contaminated soil and water through biosorbents: A review of current understanding and future challenges. *Physiol. Plant.* **2021**, *173*, 394–417. [CrossRef] [PubMed]
2. Yılmaz, A.B.; Yanar, A.; Alkan, E.N. Review of heavy metal accumulation on aquatic environment in Northern East Mediterrenean Sea part I: Some essential metals. *Rev. Environ. Health* **2017**, *32*, 119–163. [CrossRef] [PubMed]
3. Tchounwou, P.B.; Yedjou, C.G.; Patlolla, A.K.; Sutton, D.J. Heavy metal toxicity and the environment. *Exp. Suppl.* **2012**, *101*, 133–164. [PubMed]
4. Mudd, G.M. Global trends and environmental issues in nickel mining: Sulfides versus laterites. *Ore Geol. Rev.* **2010**, *38*, 9–26. [CrossRef]
5. Park, I.; Tabelin, C.B.; Jeon, S.; Li, X.; Seno, K.; Ito, M.; Hiroyoshi, N. A review of recent strategies for acid mine drainage prevention and mine tailings recycling. *Chemosphere* **2019**, *219*, 588–606. [CrossRef] [PubMed]
6. Azizi, S.; Kamika, I.; Tekere, M. Evaluation of Heavy Metal Removal from Wastewater in a Modified Packed Bed Biofilm Reactor. *PLoS ONE* **2016**, *11*, e0155462. [CrossRef] [PubMed]
7. Huang, C.; Huang, C.P. Application of *Aspergillus oryze* and *Rhizopus oryzae* for Cu^{2+} removal. *Water Res.* **1996**, *30*, 1985–1990. [CrossRef]
8. Ayangbenro, A.S.; Babalola, O.O. A New Strategy for Heavy Metal Polluted Environments: A Review of Microbial Biosorbents. *Int. J. Environ. Res. Public Health* **2017**, *14*, 94. [CrossRef]
9. Oyewole, O.A.; Zobeashia, S.S.L.T.; Oladoja, E.O.; Raji, R.O.; Odiniya, E.E.; Musa, A.M. Biosorption of heavy metal polluted soil using bacteria and fungi isolated from soil. *SN Appl. Sci.* **2017**, *1*, 857. [CrossRef]
10. Gadd, G.M. Biosorption: Critical review of scientific rationale, environmental importance and significance for pollution treatment. *J. Chem. Technol. Biotechnol.* **2009**, *84*, 13–28. [CrossRef]
11. Monge-Amaya, O.; Certucha-Barragán, M.T.; Almendariz-Tapia, F.J.; Figueroa-Torres, G.M. Removal of Heavy Metals from Aqueous Solutions by Aerobic and Anaerobic Biomass. In *Biomass Production and Uses*; IntechOpen: London, UK, 2015.
12. Rumo, C.; Stein, A.; Klehr, J.; Tachibana, R.; Prescimone, A.; Häussinger, D.; Ward, T.R. An Artificial Metalloenzyme Based on a Copper Heteroscorpionate Enables sp3 C–H Functionalization via Intramolecular Carbene Insertion. *J. Am. Chem. Soc.* **2022**, *144*, 11676–11684. [CrossRef] [PubMed]
13. Facchetti, G.; Rimoldi, I. 8-Amino-5,6,7,8-tetrahydroquinoline in iridium(iii) biotinylated Cp* complex as artificial imine reductase. *New J. Chem.* **2018**, *42*, 18773–18776. [CrossRef]
14. Pellegrino, S.; Facchetti, G.; Contini, A.; Gelmi, M.L.; Erba, E.; Gandolfi, R.; Rimoldi, I. Ctr-1 Mets7 motif inspiring new peptide ligands for Cu(i)-catalyzed asymmetric Henry reactions under green conditions. *RSC Adv.* **2016**, *6*, 71529–71533. [CrossRef]
15. Vermaak, V.; Vosloo, H.C.M.; Swarts, A.J. Fast and Efficient Nickel(II)-catalysed Transfer Hydrogenation of Quinolines with Ammonia Borane. *Adv. Synth. Catal.* **2020**, *362*, 5788–5793. [CrossRef]
16. Li, B.; Chen, J.; Zhang, Z.; Gridnev, I.D.; Zhang, W. Nickel-Catalyzed Asymmetric Hydrogenation of N-Sulfonyl Imines. *Angew. Chem. Int. Ed.* **2019**, *58*, 7329–7334. [CrossRef] [PubMed]
17. Qin, H.; Hu, T.; Zhai, Y.; Lu, N.; Aliyeva, J. The improved methods of heavy metals removal by biosorbents: A review. *Environ. Pollut.* **2020**, *258*, 113777. [CrossRef]
18. Sutherland, C.; Venkobachar, C. A diffusion-chemisorption kinetic model for simulating biosorption using forest macrofungus, *Fomes fasciatus*. *Int. Res. J. Plant Sci.* **2010**, *1*, 107–117.
19. Teng, Z.; Shao, W.; Zhang, K.; Huo, Y.; Zhu, J.; Li, M. Pb biosorption by *Leclercia adecarboxylata*: Protective and immobilized mechanisms of extracellular polymeric substances. *Chem. Eng. J.* **2019**, *375*, 122113. [CrossRef]
20. Sag, Y.; Kutsal, T. Recent trends in the biosorption of heavy metals: A review. *Biotechnol. Bioprocess. Eng.* **2001**, *6*, 376. [CrossRef]
21. Wang, J.; Chen, C. Biosorbents for heavy metals removal and their future. *Biotechnol. Adv.* **2009**, *27*, 195–226. [CrossRef]
22. Wang, L.L.; Wang, L.F.; Ren, X.M.; Ye, X.D.; Li, W.W.; Yuan, S.J.; Sun, M.; Sheng, G.P.; Yu, H.Q.; Wang, X.K. pH Dependence of Structure and Surface Properties of Microbial EPS. *Environ. Sci. Technol.* **2012**, *46*, 737–744. [CrossRef] [PubMed]
23. De Philippis, R.; Micheletti, E. Heavy metal removal with exopolysaccharide-producing cyanobacteria. *Heavy Met. Environ.* **2009**, *29*, 89–122.
24. Vishan, I.; Kalamdhad, A.S. Heavy metal removal through bacterial biomass isolated from various contaminated sites. *Int. J. Environ. Sci.* **2016**, *7*, 1–18.
25. Sadouk, A.; Mergeay, M. Chromosome mapping in *Alkaligens eutrophus* CH34. *Mol. Gen. Genet.* **1993**, *240*, 181–187. [CrossRef] [PubMed]
26. Morgan, J.W.; Forster, C.F.; Evison, L. A comparative study of the nature of biopolymers extracted from anaerobic and activated sludge. *Water Res.* **1990**, *24*, 743–750. [CrossRef]
27. Xia, L.; Zheng, X.L.; Shao, H.B.; Xin, J.; Sun, Z.Y.; Wang, L.Y. Effects of bacterial cells and two types of extracellular polymers on bioclogging of sand columns. *J. Hydrol.* **2016**, *535*, 293–300. [CrossRef]
28. Dreywood, R. Qualitative test for carbohydrate material. *Ind. Eng. Chem.* **1946**, *18*, 499. [CrossRef]
29. Bradford, M. A rapid and sensitive method for the quantitation of microgram quantities of protein utilizing the principle of protein-dye binding. *Anal. Biochem.* **1976**, *72*, 248–254. [CrossRef]

30. Crini, G.; Peindy, H.N.; Gimbert, F.; Robert, C. Removal of C.I. Basic Green 4 (Malachite Green) from aqueous solutions by adsorption using cyclodextrin-based adsorbent: Kinetic and equilibrium studies. *Sep. Purif. Technol.* **2007**, *53*, 97–110. [CrossRef]

31. Lacerda, E.C.M.; dos Passos Galluzzi Baltazar, M.; dos Reis, T.A.; do Nascimento, C.A.O.; Côrrea, B.; Jandelli Gimenes, L. Copper biosorption from an aqueous solution by the dead biomass of *Penicillium ochrochloron*. *Env. Monit. Assess.* **2019**, *191*, 247. [CrossRef]

32. Jiang, L.; Zhou, W.; Liu, D.; Liu, T.; Wang, Z. Biosorption isotherm study of Cd^{2+}, Pb^{2+} and Zn^{2+} biosorption onto marine bacterium *Pseudoalteromonas sp*. SCSE709-6 in multiple systems. *J. Mol. Liq.* **2017**, *247*, 230–237. [CrossRef]

33. Gandolfi, R.; Facchetti, G.; Cavalca, L.; Mazzini, S.; Colombo, M.; Coffetti, G.; Borgonovo, G.; Scaglioni, L.; Zecchin, S.; Rimoldi, I. Hybrid Catalysts from Copper Biosorbing Bacterial Strains and Their Recycling for Catalytic Application in the Asymmetric Addition Reaction of B2(pin)2 on α,β-Unsaturated Chalcones. *Catalysts* **2022**, *12*, 433. [CrossRef]

34. Facchetti, G.; Bucci, R.; Fusè, M.; Rimoldi, I. Asymmetric Hydrogenation vs. Transfer Hydrogenation in the Reduction of Cyclic Imines. *ChemistrySelect* **2018**, *3*, 8797–8800. [CrossRef]

35. Hong, T.; Yin, J.Y.; Nie, S.P.; Xie, M.Y. Applications of infrared spectroscopy in polysaccharide structural analysis: Progress, challenge and perspective. *Food Chem. X* **2021**, *12*, 100168. [CrossRef] [PubMed]

36. Fang, L.; Yang, S.; Huang, Q.; Xue, A.; Cai, P. Biosorption mechanisms of Cu(II) by extracellular polymeric substances from *Bacillus subtilis*. *Chem. Geol.* **2014**, *386*, 143–151. [CrossRef]

37. Rajeswari Kulkarni, M.; Vidya Shetty, K.; Srinikethan, G. Kinetic and equilibrium modeling of biosorption of nickel (II) and cadmium (II) on brewery sludge. *Water Sci. Technol.* **2019**, *79*, 888–894. [CrossRef]

38. Nagarajan, N.; Gunasekaran, P.; Rajendran, P. Genetic characterization, nickel tolerance, biosorption, kinetics, and uptake mechanism of a bacterium isolated from electroplating industrial effluent. *Can. J. Microbiol.* **2015**, *61*, 297–306. [CrossRef]

39. Bhainsa, K.C.; D'Souza, S.F. Removal of copper ions by the filamentous fungus, *Rhizopus oryzae* from aqueous solution. *Bioresour. Technol.* **2008**, *99*, 3829–3835. [CrossRef]

40. Verma, A.; Shalu Singh, A.; Bishnoi, N.R.; Gupta, A. Biosorption of Cu (II) using free and immobilized biomass of *Penicillium citrinum*. *Ecol. Eng.* **2013**, *61*, 486–490. [CrossRef]

41. Sethuraman, P.; Dharmendira Kumar, M. Biosorption Kinetics of Cu (II) Ions Removal from Aqueous Solution using Bacteria. *Pak. J. Biol. Sci.* **2011**, *14*, 327–335. [CrossRef]

42. Kashyap, S.; Chandra, R.; Kumar, B.; Verma, P. Biosorption efficiency of nickel by various endophytic bacterial strains for removal of nickel from electroplating industry effluents: An operational study. *Ecotoxicology* **2021**, *31*, 565–580. [CrossRef] [PubMed]

43. Dursun, A.Y. A comparative study on determination of the equilibrium, kinetic and thermodynamic parameters of biosorption of copper(II) and lead(II) ions onto pretreated *Aspergillus niger*. *Biochem. Eng. J.* **2006**, *28*, 187–195. [CrossRef]

44. Puyen, Z.M.; Villagrasa, E.; Maldonado, J.; Diestra, E.; Esteve, I.; Solé, A. Biosorption of lead and copper by heavy-metal tolerant *Micrococcus luteus* DE2008. *Bioresour. Technol.* **2012**, *126*, 233–237. [CrossRef] [PubMed]

45. Akhter, K.; Ghous, T.; Andleeb, S.; Ejaz, S.; Khan, B.A.; Ahmed, M.N. Bioaccumulation of heavy metals by metal-resistant bacteria isolated from *Tagetes minuta* rhizosphere, growing in soil adjoining automobile workshops. *Pak. J. Zool.* **2017**, *49*, 1841–1846. [CrossRef]

46. Naskar, A.; Bera, D. Mechani.istic exploration of Ni (II) removal by immobilized bacterial biomass and interactive influence of coexisting surfactants. *Environ. Prog. Sustain. Energy* **2018**, *37*, 342–354. [CrossRef]

47. Gheethi, A.A.; Efaq, A.N.; Mohamed, R.M.; Abdel-Monem, M.O.; Abdullah, A.H.; Amir Hashim, M.K. Bio-removal of Nickel ions by *Sporosarcina pasteurii* and *Bacillus megaterium*, a Comparative Study. *IOP Conf. Ser. Mater. Sci. Eng.* **2017**, *226*, 012044. [CrossRef]

48. Gadd, G.M. Heavy metal accumulation by bacteria and other microorganisms. *Experientia* **1990**, *46*, 834–840. [CrossRef]

49. Díaz, A.; Marrero, J.; Cabrera, G.; Coto, O.; Gómez, J.M. Biosorption of nickel, cobalt, zinc and copper ions by *Serratia marcescens* strain 16 in mono and multimetallic systems. *Biodegradation* **2022**, *33*, 33–43. [CrossRef]

50. Cristani, M.; Naccari, C.; Nostro, A.; Pizzimenti, A.; Trombetta, D.; Pizzimenti, F. Possible use of *Serratia marcescens* in toxic metal biosorption (removal). *Env. Sci. Pollut. Res.* **2012**, *19*, 161–168. [CrossRef] [PubMed]

51. Li, Y.; Li, Q.; Wu, C.; Luo, X.; Yu, X.; Chen, M. The inappropriate application of the regression Langmuir Qm for adsorption capacity comparison. *Sci. Total Environ.* **2020**, *699*, 134222. [CrossRef] [PubMed]

52. Wang, J.; Guo, X. Adsorption isotherm models: Classification, physical meaning, application and solving method. *Chemosphere* **2020**, *258*, 127279. [CrossRef] [PubMed]

53. Tran, H.N.; You, S.-J.; Hosseini-Bandegharaei, A.; Chao, H.-P. Mistakes and inconsistencies regarding adsorption of contaminants from aqueous solutions: A critical review. *Water Res.* **2017**, *120*, 88–116. [CrossRef] [PubMed]

54. Fang, L.C.; Wei, X.; Cai, P.; Huang, Q.Y.; Chen, H.; Liang, W.; Rong, X.M. Role of extracellular polymeric substances in Cu(II) adsorption on *Bacillus subtilis* and *Pseudomonas putida*. *Bioresour. Technol.* **2011**, *102*, 1137–1141. [CrossRef] [PubMed]

55. Hao, L.K.; Guo, Y.; Byrne, J.M.; Zeitvogel, F.; Schmid, G.; Ingino, P.; Li, J.L.; Neu, T.R.; Swanner, E.D.; Kappler, A.; et al. Binding of heavy metal ions in aggregates of microbial cells, EPS and biogenic iron minerals measured in-situ using metal- and glycoconjugates-specific fluorophores. *Geochim. Cosmochim. Acta* **2016**, *180*, 66–96. [CrossRef]